Spectrally encoded angular light scattering

Jost Adam,[1,2,*] **Ata Mahjoubfar,**[1,2] **Eric D. Diebold,**[1,2] **Brandon W. Buckley,**[1,2] **and Bahram Jalali**[1,2,3,4]

[1] *Department of Electrical Engineering, University of California, Los Angeles, CA 90095, USA*
[2] *California NanoSystems Institute, Los Angeles, CA 90095, USA*
[3] *Department of Bioengineering, University of California, Los Angeles, CA 90095, USA*
[4] *Department of Surgery, David Geffen School of Medicine, University of California, Los Angeles, CA 90095, USA*
[*] *jost@ucla.edu*

Abstract: The angular light scattering profile of microscopic particles significantly depends on their morphological parameters, such as size and shape. This dependency is widely used in state-of-the-art flow cytometry methods for particle classification. We introduce a new spectrally encoded angular light scattering method, with potential application in scanning flow cytometry. We show that a one-to-one wavelength-to-angle mapping enables the measurement of the angular dependence of scattered light from microscopic particles over a wide dynamic range. Improvement in dynamic range is obtained by equalizing the angular dependence of scattering via wavelength equalization. Continuous angular spectrum is obtained without mechanical scanning enabling single-shot measurement. Using this information, particle morphology can be determined with improved accuracy. We derive and experimentally verify an analytic wavelength-to-angle mapping model, facilitating rapid data processing. As a proof of concept, we demonstrate the method's capability of distinguishing differently sized polystyrene beads. The combination of this technique with time-stretch dispersive Fourier transform offers real-time and high-throughput (high frame rate) measurements and renders the method suitable for integration in standard flow cytometers.

OCIS codes: (290.5820) Scattering measurements; (290.4020) Mie theory; (290.5850) Scattering, particles; (170.7160) Ultrafast technology; (170.1530) Cell analysis; (170.3890) Medical optics instrumentation.

References and links

1. D. Davies, *Flow Cytometry: Principles and Applications* (Humana, 2007, chap. Cell Sorting by Flow Cytometry).
2. R. Drezek, A. Dunn, and R. Richards-Kortum, "Light scattering from cells: finite-difference time-domain simulations and goniometric measurements," Appl. Opt. **38**, 3651–3661 (1999).
3. V. P. Maltsev, "Scanning flow cytometry for individual particle analysis," Rev. Sci. Instrum. **71**(1), 243–255 (2000).
4. K. Singh, C. Capjack, W. Rozmus, and C. Backhouse, "Reply [Analysis of cellular structure by light scattering measurements in a new cytometer design based on a liquid-core waveguide]," IEE Proc. Nanobiotechnol. **153**(5), 135–135 (2006).
5. J. Chou, D. R. Solli, and B. Jalali, "Real-time spectroscopy with subgigahertz resolution using amplified dispersive Fourier transformation," Appl. Phys. Lett. **92**(11), 111102 (2008).

#197419 - $15.00 USD Received 9 Sep 2013; revised 14 Oct 2013; accepted 16 Oct 2013; published 15 Nov 2013

6. K. Goda, A. Ayazi, D. R. Gossett, J. Sadasivam, C. K. Lonappan, E. Sollier, A. M. Fard, S. C. Hur, J. Adam, C. Murray, C. Wang, N. Brackbill, D. Di Carlo, and B. Jalali, "High-throughput single-microparticle imaging flow analyzer," Proc. Natl. Acad. Sci. USA **109**(29), 11630–11635 (2012).
7. K. Goda, A. Mahjoubfar, C. Wang, A. Fard, J. Adam, D. Gossett, A. Ayazi, E. Sollier, O. Malik, E. Chen, Y. Liu, R. Brown, N. Sarkhosh, D. Di Carlo, and B. Jalali, "Hybrid dispersion laser scanner," Sci. Rep. **2**, 445 (2012).
8. K. Goda, D. R. Solli, and B. Jalali, "Real-time optical reflectometry enabled by amplified dispersive Fourier transformation," Appl. Phys. Lett. **93**(3), 031106 (2008).
9. K. Goda, D. R. Solli, K. K. Tsia, and B. Jalali, "Theory of amplified dispersive Fourier transformation," Phys. Rev. A **80**(4), 043821 (2009).
10. K. Goda, K. K. Tsia, and B. Jalali, "Serial time-encoded amplified imaging for real-time observation of fast dynamic phenomena," Nature **458**(7242), 1145–1149 (2009).
11. A. Mahjoubfar, C. Chen, K. R. Niazi, S. Rabizadeh, and B. Jalali, "Label-free high-throughput cell screening in flow," Biomed. Opt. Express **4**(9), 1618 (2013).
12. D. Solli, G. Herink, B. Jalali, and C. Ropers, "Fluctuations and correlations in modulation instability," Nat. Photon. **6**(7), 463–468 (2012).
13. B. Wetzel, A. Stefani, L. Larger, P. Lacourt, J. Merolla, T. Sylvestre, A. Kudlinski, A. Mussot, G. Genty, F. Dias, and J. M. Dudley, "Real-time full bandwidth measurement of spectral noise in supercontinuum generation," Sci. Rep. **2**, 882 (2012).
14. E. Hecht, *Optics*, 4th ed. (Addison Wesley, 2001).
15. Bangs Laboratories, Inc., "Fluorescent polymer mircrospheres," http://www.bangslabs.com. Accessed: 09/06/2013.
16. G. Mie, "Beiträge zur Optik trüber Medien, speziell kolloidaler Metallösungen," Ann. Phys. **330**, 377–445 (1908).
17. J. A. Stratton, *Electromagnetic Theory* (McGraw Hill, 1941).
18. G. Agrawal, *Nonlinear Fiber Optics*, 3rd ed. (Academic, 2001).
19. K. Goda and B. Jalali, "Dispersive Fourier transformation for fast continuous single-shot measurements," Nat. Photon. **7**(2), 102–112 (2013).
20. P. Kelkar, F. Coppinger, A. Bhushan, and B. Jalali, "Time-domain optical sensing," Electron. Lett. **35**(19), 1661–1662 (1999).
21. M. A. Muriel, J. Azaña, and A. Carballar, "Real-time Fourier transformer based on fiber gratings," Opt. Lett. **24**(1), 1–3 (1999).
22. E. D. Diebold, N. K. Hon, Z. W. Tan, J. Chou, T. Sienicki, C. Wang, and B. Jalali, "Giant tunable optical dispersion using chromo-modal excitation of a multimode waveguide," Opt. Express **19**(24), 23809–23817 (2011).

1. Introduction

Standard light scattering instruments, such as flow cytometers, illuminate individual particles (in flow) with a laser beam and measure the scattered light at two fixed, forward and side, angles. From these two measurements, a scatter bivariate plot, called a cytogram, is created and particles are classified based on the corresponding locations on this plot (See for example: [1]). For accurate particle classification, one needs to obtain morphological information about particles, such as size, refractive index, shape etc. To this end, one needs to measure the angular dependency, i.e. the entire angular spectrum of the scattered light [2]. This so called scanning flow cytometry (SFC) is usually done by mechanical scanning (goniometric approach), flying light scattering indicatrix method (FLSI) [3], or a liquid-core-waveguide based approach [4]. One problem with all flow cytometers is the low count of side scattered photons. The exponential drop in the number of scattered photons with angle away from the forward direction limits the range of angles over which the angular dependence can be measured. The large difference (exponentially varying) in light intensity between the forward and side scattered angles results in a prohibitively large dynamic range requirement on the detection system. Hence, in conventional flow cytometry, different detectors with various sensitivities are required for each angle. Mechanically scanning flow cytometers on the other hand, must keep the particles at a fixed position during measurement of the scattered light angular spread. This not only complicates the system but more importantly prevents high throughput real-time cell or particle screening. While FLSI mitigates this, it requires special and complex flow channel engineering, in which light is coupled into the flow channel, propagating collinearly with the cells. More importantly,

problem being solved

#197419 - $15.00 USD Received 9 Sep 2013; revised 14 Oct 2013; accepted 16 Oct 2013; published 15 Nov 2013

it suffers from the low count of side-scattered photons and the large dynamic range between the forward and side scattered photon count. Our spectrally encoded angular light scattering (SEALS) technique overcomes this dynamic range limitation. It illuminates a particle with a focused rainbow of light, i.e. light with an angle-dependent wavelength, and derives the angle-dependent scattering profile by analyzing the scattered spectrum at a fixed angle. As a result, SEALS captures the angular dependency of scattered light continuously over a broad angular range, leading to more morphological information about the cell or particle. Since this continuous angular scattering measurement only requires a single photo detector, it comprises simple light collection optics and no need for specialized flow channels. When combined with time-stretch dispersive Fourier transform, previously utilized for high-speed imaging, reflectometry, spectroscopy and cell screening [5–10], SEALS offers far higher real-time throughput than conventional techniques. Therefore it is capable of detecting rare abnormal particles (such as cells) in a large population of normal particles (such as cells) with good statistical accuracy. Its fast shutter speed freezes the cell motion and rotation hence eliminating the need to keep the cell in a fixed position as required in conventional SFC.

1. Setup math and " semi-analytical" base
2. Analytically characterize system's ang. resolution??? w.r.t. detectors appy

This article is structured as follows. In the succeeding section we describe the proposed angular spectral scanning concept and the proof of principle experimental setup. In section 3 we first develop the semi-analytical base for the wavelength-to-angle mapping and verify the outcome with experimental data and ray tracing simulations. Second, we analytically characterize the system's angular resolution with respect to the detector aperture and the target-to-probe distance. We then state our experimental findings regarding particle classification. We provide an outlook to high-throughput implementations in section 4 and conclude the manuscript in the final section.

2. Equalization of angular dependence and experimental setup

A pulsed mode-locked laser produces pulses with a relatively broad spectrum (about 20 nm bandwidth), centered at 1590 nm, as shown in the system block diagram (Fig. 1). The pulse power spectrum is subsequently modified with a tunable optical filter to provide more power to optical frequencies corresponding to side scattering angles. This in effect equalizes the angular dependence of scattering, increasing the photon count at side scattering angles and reducing the required dynamic range of the detection circuitry. Next, a pair of diffraction gratings converts the broadband optical pulse into a collimated one-dimensional rainbow. In our proof of principle experiment, we managed to achieve wavelength equalization (and hence angular equalization) by using a quarter- and a half-wave plate together with the double-grating setup. Subsequently, a high numerical aperture (NA) objective lens (60×, NA= 0.7) focuses the resulting one-dimensional rainbow onto particles under test. Following the double-grating arrangement, a telescope setup, comprising two gold-coated parabolic mirrors shrinks the beam size to match the objective lens entrance pupil diameter [11]. The objective lens thereby converts the optical wavelengths contained in each broadband pulse to an angular rainbow. A microscopic particle, located at the objective lens' focal point, subsequently scatters the incident angular rainbow. As a consequence, by measuring the scattered intensity spectrum at any point in the plane of incidence, the full angular scattering profile can be revealed. The particle is hence illuminated by light at different angles and it is sufficient to measure the scattered light at a single, arbitrary angle with appropriate signal-to-noise ratio. This procedure maps the actual scattering angle into wavelength (optical frequency), and scattering patterns can be analyzed by simply examining the resulting spectral intensities. In the 1550 nm regime, the 20 nm optical bandwidth (1.3 % fractional bandwidth) is sufficiently narrow such that wavelength dependence of scattering can be neglected. As for our proof of concept experiment, in order to measure the spectrum, we fed the output directly into an optical spectrum analyzer (OSA) via a multimode fiber. This spec-

#197419 - $15.00 USD Received 9 Sep 2013; revised 14 Oct 2013; accepted 16 Oct 2013; published 15 Nov 2013

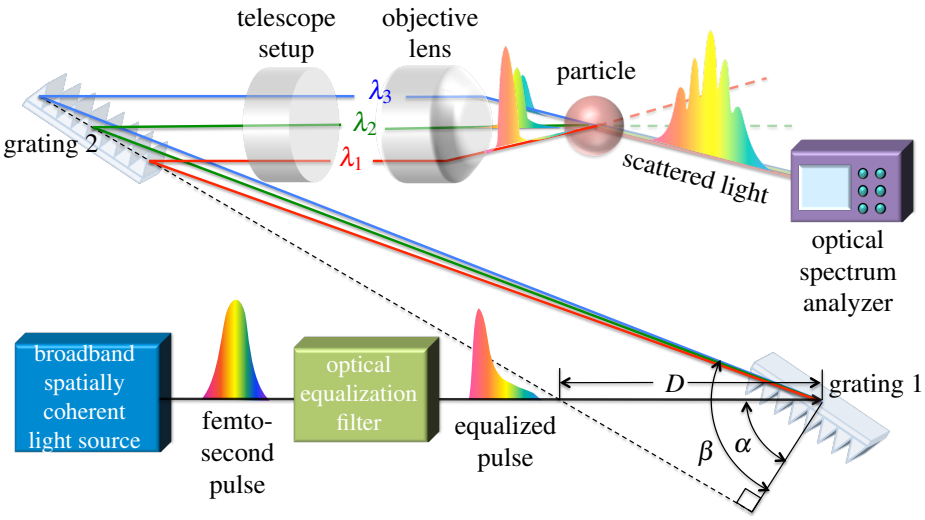

Fig. 1. An optical pulse is created by a broadband pulsed laser. The power spectrum of the illuminating light is modified with an optical filter to provide more power to optical frequencies corresponding to side scattering angles. Next, the broadband optical pulse is converted into a collimated one-dimensional rainbow using a pair of diffraction gratings. A telescope setup is used to adjust the beam size. The resulting one-dimensional rainbow is focused onto particles under test, by a high-NA objective lens (60x, NA=0.7). The particle is hence illuminated by light at different angles and scattered light is measured at a single, fixed angle. The output is then directly fed into an optical spectrum analyzer (OSA) via a multimode fiber.

tral measurement, however, can also be performed in a real-time by a time-stretch dispersive Fourier transform setup [6, 12, 13].

3. Wavelength-to-angle mapping and bead separation

The proposed technique is based on focusing the incident light onto the particles under test. In conventional flow cytometry this focusing principle is not feasible, since it would lead to a high amount of unwanted angular ambiguity at the side scattering detector. Hence, this is only possible with respect to the existence of a distinct (one-to-one) wavelength-to-angle mapping, providing unique scattering information over a broad angular range. This wavelength-to-angle mapping is carried out as a two-step process. First, a pair of parallel diffraction gratings, with equal groove spacing, spatially disperses an optical laser pulse. This results in a collimated beam comprising a specific beam displacement for each input wavelength. As a second step, this beam displacement is converted to angle by focusing the beam with an objective lens. In the following we investigate this mapping's behavior by an analytical, numerical, and experimental characterization. We demonstrate that the proposed mapping can be completely analytically treated with a once found set of static system parameters. We further provide a brief discussion on the system's angular resolution and close this section with an experimental demonstration of bead separability. According to the grating equation [14], combined with a straight-forward geometric calculation, the beam displacement y relates to the beam wavelength λ via

$$y(\lambda) = -M\frac{D\tan(\alpha-\beta)}{1+\tan(\alpha-\beta)\tan(\alpha)}, \tag{1}$$

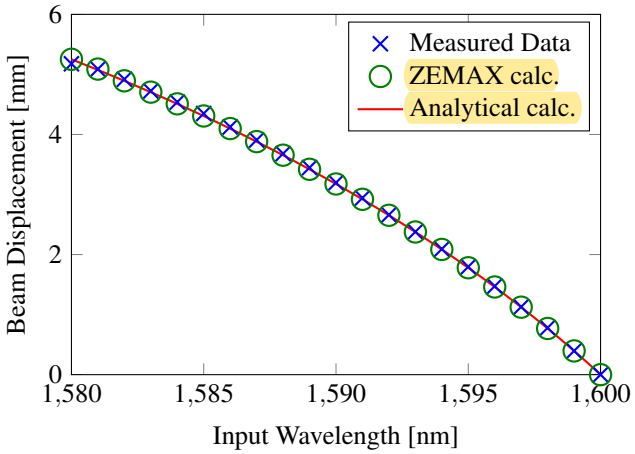

Fig. 2. The wavelength-to-beam-displacement mapping shows the agreement between measured data, ray tracing simulations and analytic calculations.

where the incident beam angle α and the diffracted beam angle $\beta = \sin^{-1}(m\lambda/d - \sin(\alpha))$ are given with respect to the grating surface normal. Furthermore, D is the distance between the gratings along the incident beam (x-)direction, m is the diffraction order (usually set to 1, since the gratings are operated in first order diffraction mode) and d represents the grating groove spacing. Since the grating pair is followed by a telescope setup to widen up or shrink the beam, the beam displacement is further multiplied by a magnification factor M. The experimental realization contains a telescope setup with two commercially available parabolic mirrors, revealing a magnification factor $M = 1/6$. The resulting spatial beam width consequently reads $y(\lambda_{\text{min}}) - y(\lambda_{\text{max}})$ and the beam center is located at $y_{\text{center}} = (y(\lambda_{\text{min}}) - y(\lambda_{\text{max}}))/2$. As for the second mapping step, the beam displacement is converted to angle by focusing the beam with an objective lens. Assuming that the objective lens can be modeled as a single lens, another straight forward geometric calculation leads to the wavelength-to-angle mapping

$$\theta(\lambda) = \tan^{-1}\left(\frac{2}{P}\left(y(\lambda) - y_{\text{center}} + d_{\text{corr}}\right)\tan(\sin^{-1}(NA))\right), \tag{2}$$

where P is the objective lens entrance pupil diameter, NA is the objective lens numerical aperture (NA) and d_{corr} is a correction term representing potential beam center (y-) misalignment with respect to the objective lens entrance pupil diameter P. In order to characterize the actual wavelength-to-displacement mapping, we measured the resulting $y(\lambda)$-displacement of the collimated rainbow beam with a beam profiler. Concurrently, we performed ray-tracing simulations (ZEMAX) according to the experimental parameters and used the same parameters to calculate $y(\lambda)$ via Eq. (1). Figure 2 demonstrates the agreement between measurement, simulation and analytic calculation. We measured the experimental setup's characteristic wavelength-to-angle mapping with a continuous wave (CW) laser source and a rotational stage holding an optical multimode fiber tip, in combination with an optical spectrum analyzer (OSA). The analytic expression in Eq. (2) was fitted to the measurement results. To this end we started with actual measured optical setup dimensions, only using the entrance pupil diameter P and the correction factor d_{corr} as variable fitting parameters. The result is shown in Fig. 3, demonstrating the agreement between the measured data and the analytic calculation obtained by employing Eqs. (1) and (2). As a consequence, with once found system parameters D, α and NA, and fitting parameters P and d_{corr} , the proposed wavelength-to-angle mapping can be treated entirely

#197419 - $15.00 USD Received 9 Sep 2013; revised 14 Oct 2013; accepted 16 Oct 2013; published 15 Nov 2013

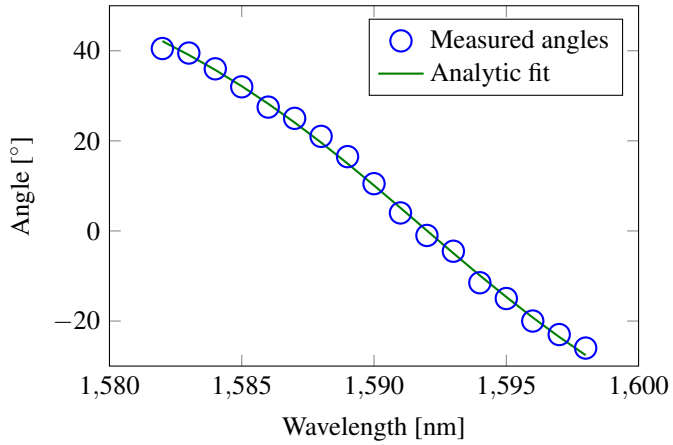

Fig. 3. The wavelength-to-angle mapping measurement shows the agreement with the analytic calculation obtained by employing Eqs. (1) and (2), with the entrance pupil diameter P and the correction factor d_{corr} as the only variable fitting parameters.

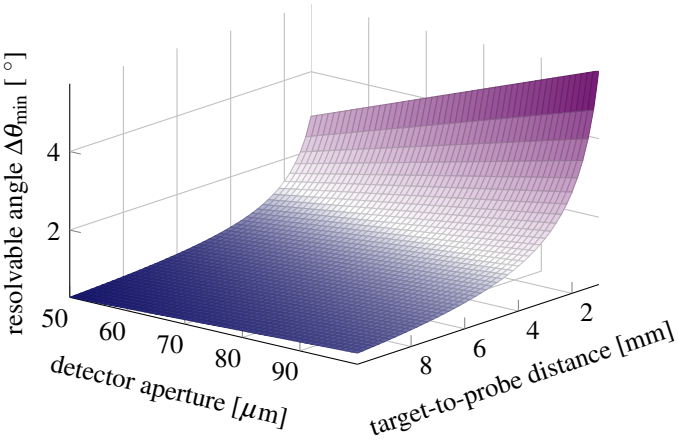

Fig. 4. Minimum resolvable angle $\Delta\theta$ (in degrees) with respect to typical detector aperture (or fiber core diameter) values d and the probe-to-target distance L. The white area corresponds to $\Delta\theta = 1°$.

analytically.

Since, due to the high-NA objective lens, the light behind the target is widely spread, the system's angular resolution is calculated by taking into account the detector aperture diameter d and the distance L between the fiber tip and the target. A straightforward geometric consideration leads to the minimal resolvable angle $\Delta\theta_{\mathrm{min}} = 2\tan^{-1}(d/(2L))$ With respect to typical fiber core diameter values d (50 μm to 100 μm) and probe-to-target distances L (2 mm to 10 mm), a realistic minimal resolvable angle of approximately one degree is found. (Fig. 4). Furthermore, the diffraction grating wavelength resolvability, $d\lambda$, may be calculated via $d\lambda = \lambda_0 d/(2mw_0)$, where $\lambda_0 = 1590\,\mathrm{nm}$ is the center wavelength, the system's entrance beam waist, w_0, measures 3 mm, $d = 1100\,\mathrm{nm}$ is the grating pitch size, and $m = 1$ is the diffraction order. With these parameters, we get a wavelength resolvability of $d\lambda = 0.48\,\mathrm{nm}$, which leads to 42 resolvable scattering angles inside the provided 20 nm bandwith.

#197419 - $15.00 USD Received 9 Sep 2013; revised 14 Oct 2013; accepted 16 Oct 2013; published 15 Nov 2013

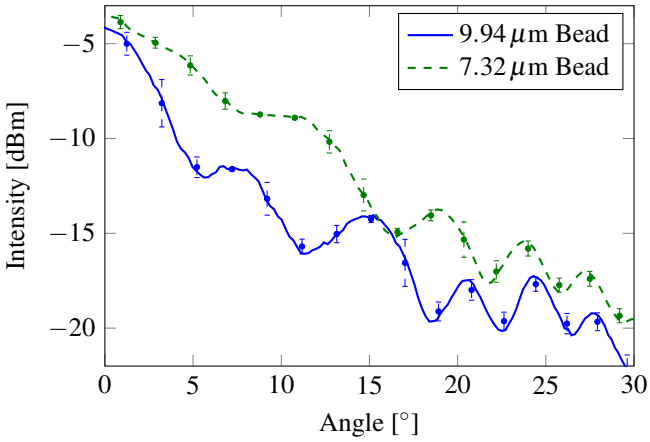

Fig. 5. Proof-of-principle measurement of the angular scattering profiles for 7.32 μm and 9.94 μm (nominal) diameter polystyrene beads, taken from single OSA traces. The error bars correspond to the angular resolvability analysis provided in section 2, while the (dashed) lines represent measurement curve fits. As opposed to conventional flow cytometers, which measure the scattering at only two points (forward- and side-scattering), SEALSperforms single shot measurement of the continuous angular spectrum. Here, the differently sized beads can easily be distinguished by their different number of scattering lobes (spatial frequencies). The additional information contained in the continuous spectrum improves particle classification [2–4].

In order to demonstrate the SEALS system's capability to separate particles with different morphology, we analyzed spherical polystyrene beads with two different sizes (7.32 μm and 9.94 μm diameters, refractive index $n = 1.39$, [15]). To this end, we wetted a 140 μm thick glass wafer with diluted bead solution and dried it on a hot plate. We aligned the center of single, isolated beads to the objective lens focal point, using a translation stage. We then measured the scattering spectra of different beads with the OSA and transformed the measured spectra into scattered angular intensity via the above-described wavelength-to-angle mapping. Our experimental results show scattering lobes similar to the prediction by Mie theory [16, 17]. In agreement with the theory, the smaller sized beads show a smaller number of lobes than the larger sized beads (Fig. 5). Consequently, we are able to distinguish beads with different morphologies based on their angular scattering profiles.

4. Discussion on high-throughput implementation

A high-throughput realization may be implemented by replacing the optical spectrum analyzer with the Time Stretch Dispersive Fourier Transform (TS-DFT). By mapping the illuminating light frequency into time and slowing the time scale, using group velocity dispersion (GVD) [18], single shot spectra can be obtained at high throughput using a photodiode and a real-time digitizer. The necessary GVD may be achieved by using a high dispersion fiber [19, 20]. Alternatively, other devices such as chirped fiber Bragg gratings (FBG) [21] or chromo-modal dispersion (CMD) [22] can be used. In order to improve the signal to noise ratio (SNR), the fiber can be pumped with diode pump lasers to create optical amplification via stimulated Raman scattering [9, 19]. The amount of group velocity dispersion is chosen to time-stretch the optical pulses, that is, to slow it down, such that it may be digitized in real-time.

#197419 - $15.00 USD Received 9 Sep 2013; revised 14 Oct 2013; accepted 16 Oct 2013; published 15 Nov 2013

5. Conclusion

We have introduced a new method for spectrally encoded angular light scattering measurement (SEALS). It enables (i) single shot measurements of the continuous angular dependence of light scattered from microscopic particles, and (ii) improvement in measurement dynamic range through equalization of the angular spectrum via wavelength filtering. The SEALS technique overcomes the bottleneck associated with low count of side-scattered photons and the large dynamic range between the forward and side scattered photon count in light scattering with application to flow cytometry. This leads to more morphological information about the cell or particle. The combination of SEALS with time-stretch dispersive Fourier transform offers real-time and high-throughput (high frame rate) measurements.

Acknowledgments

J. A. gratefully acknowledges financial support by the German Research Foundation (DFG), within the project AD $400/1-1$.

#197419 - $15.00 USD Received 9 Sep 2013; revised 14 Oct 2013; accepted 16 Oct 2013; published 15 Nov 2013